

## VU Research Portal

### Measurement of Longitudinal Spin Transfer to Lambda Hyperons in Deep Inelastic Lepton Scattering.

Airapetian, A.; van den Brand, J.F.J.; Bulten, H.J.; Simani, M.C.

**published in**

Physical Review D  
2001

**DOI (link to publisher)**

[10.1103/PhysRevD.64.112005](https://doi.org/10.1103/PhysRevD.64.112005)

**document version**

Publisher's PDF, also known as Version of record

[Link to publication in VU Research Portal](#)

**citation for published version (APA)**

Airapetian, A., van den Brand, J. F. J., Bulten, H. J., & Simani, M. C. (2001). Measurement of Longitudinal Spin Transfer to Lambda Hyperons in Deep Inelastic Lepton Scattering. *Physical Review D*, 64, 112005. <https://doi.org/10.1103/PhysRevD.64.112005>

**General rights**

Copyright and moral rights for the publications made accessible in the public portal are retained by the authors and/or other copyright owners and it is a condition of accessing publications that users recognise and abide by the legal requirements associated with these rights.

- Users may download and print one copy of any publication from the public portal for the purpose of private study or research.
- You may not further distribute the material or use it for any profit-making activity or commercial gain
- You may freely distribute the URL identifying the publication in the public portal ?

**Take down policy**

If you believe that this document breaches copyright please contact us providing details, and we will remove access to the work immediately and investigate your claim.

**E-mail address:**

[vuresearchportal.ub@vu.nl](mailto:vuresearchportal.ub@vu.nl)

**Measurement of longitudinal spin transfer to  $\Lambda$  hyperons in deep-inelastic lepton scattering**

A. Airapetian,<sup>31</sup> N. Akopov,<sup>31</sup> M. Amarian,<sup>26,31</sup> E. C. Aschenauer,<sup>6</sup> H. Avakian,<sup>10</sup> R. Avakian,<sup>31</sup> A. Avetissian,<sup>31</sup> B. Bains,<sup>15</sup> C. Baumgarten,<sup>22</sup> M. Beckmann,<sup>12</sup> S. Belostotski,<sup>25</sup> J. E. Belz,<sup>27,28</sup> Th. Benisch,<sup>8</sup> S. Bernreuther,<sup>8</sup> N. Bianchi,<sup>10</sup> J. Blouw,<sup>24</sup> H. Böttcher,<sup>6</sup> A. Borissov,<sup>5,14</sup> M. Bouwhuis,<sup>15</sup> J. Brack,<sup>4</sup> S. Brauksiepe,<sup>12</sup> B. Braun,<sup>8,22</sup> B. Bray,<sup>3</sup> S. Brons,<sup>6,28</sup> W. Brückner,<sup>14</sup> A. Brüll,<sup>14,19</sup> E. E. W. Bruins,<sup>19</sup> H. J. Bulten,<sup>24,30</sup> G. P. Capitani,<sup>10</sup> P. Carter,<sup>3</sup> P. Chumney,<sup>23</sup> E. Cisbani,<sup>26</sup> G. R. Court,<sup>17</sup> P. F. Dalpiaz,<sup>9</sup> E. De Sanctis,<sup>10</sup> D. De Schepper,<sup>19</sup> E. Devitsin,<sup>21</sup> P. K. A. de Witt Huberts,<sup>24</sup> P. Di Nezza,<sup>10</sup> M. Düren,<sup>8</sup> A. Dvoredsky,<sup>3</sup> G. Elbakian,<sup>31</sup> J. Ely,<sup>4</sup> A. Fantoni,<sup>10</sup> A. Fechtchenko,<sup>7</sup> M. Ferstl,<sup>8</sup> K. Fiedler,<sup>8</sup> B. W. Filippone,<sup>3</sup> H. Fischer,<sup>12</sup> B. Fox,<sup>4</sup> J. Franz,<sup>12</sup> S. Frullani,<sup>26</sup> M.-A. Funk,<sup>5</sup> Y. Gärber,<sup>6,8</sup> H. Gao,<sup>2,15,19</sup> F. Garibaldi,<sup>26</sup> G. Gavrilov,<sup>25</sup> P. Geiger,<sup>14</sup> V. Gharibyan,<sup>31</sup> A. Golendukhin,<sup>5,22,31</sup> G. Graw,<sup>22</sup> O. Grebenioug,<sup>25</sup> P. W. Green,<sup>1,28</sup> L. G. Greeniaus,<sup>1,28</sup> C. Grosshauser,<sup>8</sup> M. Guidal,<sup>24</sup> A. Gute,<sup>8</sup> V. Gyurjyan,<sup>10</sup> J. P. Haas,<sup>23</sup> W. Haeberli,<sup>18</sup> O. Häusser,<sup>27,28,\*</sup> J.-O. Hansen,<sup>2</sup> M. Hartig,<sup>28</sup> D. Hasch,<sup>6,10</sup> F. H. Heinsius,<sup>12</sup> R. Henderson,<sup>28</sup> M. Henoch,<sup>8</sup> R. Hertenberger,<sup>22</sup> Y. Holler,<sup>5</sup> R. J. Holt,<sup>15</sup> W. Hoprich,<sup>14</sup> H. Ihssen,<sup>5,24</sup> M. Iodice,<sup>26</sup> A. Izotov,<sup>25</sup> H. E. Jackson,<sup>2</sup> A. Jgoun,<sup>25</sup> R. Kaiser,<sup>6</sup> E. Kinney,<sup>4</sup> M. Kirsch,<sup>8</sup> A. Kisselev,<sup>2,25</sup> P. Kitching,<sup>1</sup> H. Kobayashi,<sup>29</sup> N. Koch,<sup>8</sup> K. Königsmann,<sup>12</sup> M. Kolstein,<sup>24</sup> H. Kolster,<sup>22,24,30</sup> V. Korotkov,<sup>6</sup> W. Korsch,<sup>3,16</sup> V. Kozlov,<sup>21</sup> L. H. Kramer,<sup>11,19</sup> V. G. Krivokhijine,<sup>7</sup> M. Kurisuno,<sup>29</sup> G. Kyle,<sup>23</sup> W. Lachnit,<sup>8</sup> P. Lenisa,<sup>9</sup> W. Lorenzon,<sup>20</sup> N. C. R. Makins,<sup>15</sup> S. I. Manaenkov,<sup>25</sup> F. K. Martens,<sup>1</sup> J. W. Martin,<sup>19</sup> F. Masoli,<sup>9</sup> A. Mateos,<sup>19</sup> M. McAndrew,<sup>17</sup> K. McIlhany,<sup>3,19</sup> R. D. McKeown,<sup>3</sup> F. Meissner,<sup>6,22</sup> F. Menden,<sup>12</sup> A. Metz,<sup>22</sup> N. Meyners,<sup>5</sup> O. Mikloukho,<sup>25</sup> C. A. Miller,<sup>1,28</sup> M. A. Miller,<sup>15</sup> R. Milner,<sup>19</sup> A. Most,<sup>15,20</sup> V. Muccifora,<sup>10</sup> R. Mussa,<sup>9</sup> A. Nagaitsev,<sup>7</sup> Y. Naryshkin,<sup>25</sup> A. M. Nathan,<sup>15</sup> F. Neunreither,<sup>8</sup> J. M. Niczyporuk,<sup>15,19</sup> W.-D. Nowak,<sup>6</sup> M. Nupieri,<sup>10</sup> T. G. O'Neill,<sup>2</sup> R. Openshaw,<sup>28</sup> J. Ouyang,<sup>28</sup> B. R. Owen,<sup>15</sup> V. Papavassiliou,<sup>23</sup> S. F. Pate,<sup>23</sup> M. Pitt,<sup>3</sup> S. Potashov,<sup>21</sup> D. H. Potterveld,<sup>2</sup> G. Rakness,<sup>4</sup> A. Reali,<sup>9</sup> R. Redwine,<sup>19</sup> A. R. Reolon,<sup>10</sup> R. Ristinen,<sup>4</sup> K. Rith,<sup>8</sup> P. Rossi,<sup>10</sup> S. Rudnitsky,<sup>20</sup> M. Ruh,<sup>12</sup> D. Ryckbosch,<sup>13</sup> Y. Sakemi,<sup>29</sup> I. Savin,<sup>7</sup> C. Scarlett,<sup>20</sup> F. Schmidt,<sup>8</sup> H. Schmitt,<sup>12</sup> G. Schnell,<sup>23</sup> K. P. Schüller,<sup>5</sup> A. Schwind,<sup>6</sup> J. Seibert,<sup>12</sup> T.-A. Shibata,<sup>29</sup> K. Shibatani,<sup>29</sup> T. Shin,<sup>19</sup> V. Shutov,<sup>7</sup> C. Simani,<sup>24,30</sup> A. Simon,<sup>12</sup> K. Sinram,<sup>5</sup> P. Slavich,<sup>9,10</sup> M. Spengos,<sup>5</sup> E. Steffens,<sup>8</sup> J. Stenger,<sup>8</sup> J. Stewart,<sup>2,17,28</sup> U. Stösslein,<sup>6</sup> M. Sutter,<sup>19</sup> H. Tallini,<sup>17</sup> S. Taroian,<sup>31</sup> A. Terkulov,<sup>21</sup> E. Thomas,<sup>10</sup> B. Tipton,<sup>3,19</sup> M. Tytgat,<sup>13</sup> G. M. Urciuoli,<sup>26</sup> J. F. J. van den Brand,<sup>24,30</sup> G. van der Steenhoven,<sup>24</sup> R. van de Vyver,<sup>13</sup> J. J. van Hunen,<sup>24</sup> M. C. Vetterli,<sup>27,28</sup> V. Vikhrov,<sup>25</sup> M. G. Vinciter,<sup>1</sup> J. Visser,<sup>24</sup> E. Volk,<sup>14</sup> W. Wander,<sup>8,19</sup> J. Wendland,<sup>27,28</sup> S. E. Williamson,<sup>15</sup> T. Wise,<sup>18</sup> K. Woller,<sup>5</sup> S. Yoneyama,<sup>29</sup> and H. Zohrabian<sup>31</sup>

(HERMES Collaboration)

<sup>1</sup>Department of Physics, University of Alberta, Edmonton, Alberta, Canada T6G 2J1<sup>2</sup>Physics Division, Argonne National Laboratory, Argonne, Illinois 60439-4843<sup>3</sup>W. K. Kellogg Radiation Laboratory, California Institute of Technology, Pasadena, California 91125<sup>4</sup>Nuclear Physics Laboratory, University of Colorado, Boulder, Colorado 80309-0446<sup>5</sup>DESY, Deutsches Elektronen Synchrotron, 22603 Hamburg, Germany<sup>6</sup>DESY Zeuthen, 15738 Zeuthen, Germany<sup>7</sup>Joint Institute for Nuclear Research, 141980 Dubna, Russia<sup>8</sup>Physikalisches Institut, Universität Erlangen-Nürnberg, 91058 Erlangen, Germany<sup>9</sup>Istituto Nazionale di Fisica Nucleare, Sezione di Ferrara and Dipartimento di Fisica, Università di Ferrara, 44100 Ferrara, Italy<sup>10</sup>Istituto Nazionale di Fisica Nucleare, Laboratori Nazionali di Frascati, 00044 Frascati, Italy<sup>11</sup>Department of Physics, Florida International University, Miami, Florida 33199<sup>12</sup>Fakultät für Physik, Universität Freiburg, 79104 Freiburg, Germany<sup>13</sup>Department of Subatomic and Radiation Physics, University of Gent, 9000 Gent, Belgium<sup>14</sup>Max-Planck-Institut für Kernphysik, 69029 Heidelberg, Germany<sup>15</sup>Department of Physics, University of Illinois, Urbana, Illinois 61801<sup>16</sup>Department of Physics and Astronomy, University of Kentucky, Lexington, Kentucky 40506<sup>17</sup>Physics Department, University of Liverpool, Liverpool L69 7ZE, United Kingdom<sup>18</sup>Department of Physics, University of Wisconsin-Madison, Madison, Wisconsin 53706<sup>19</sup>Laboratory for Nuclear Science, Massachusetts Institute of Technology, Cambridge, Massachusetts 02139<sup>20</sup>Randall Laboratory of Physics, University of Michigan, Ann Arbor, Michigan 48109-1120<sup>21</sup>Lebedev Physical Institute, 117924 Moscow, Russia<sup>22</sup>Sektion Physik, Universität München, 85748 Garching, Germany<sup>23</sup>Department of Physics, New Mexico State University, Las Cruces, New Mexico 88003<sup>24</sup>Nationaal Instituut voor Kernfysica en Hoge-Energiefysica (NIKHEF), 1009 DB Amsterdam, The Netherlands<sup>25</sup>Petersburg Nuclear Physics Institute, St. Petersburg, Gatchina, 188350 Russia<sup>26</sup>Istituto Nazionale di Fisica Nucleare, Sezione Sanità and Physics Laboratory, Istituto Superiore di Sanità, 00161 Roma, Italy<sup>27</sup>Department of Physics, Simon Fraser University, Burnaby, British Columbia, Canada V5A 1S6<sup>28</sup>TRIUMF, Vancouver, British Columbia, Canada V6T 2A3<sup>29</sup>Department of Physics, Tokyo Institute of Technology, Tokyo 152, Japan

<sup>30</sup>*Department of Physics and Astronomy, Vrije Universiteit, 1081 HV Amsterdam, The Netherlands*<sup>31</sup>*Yerevan Physics Institute, 375036, Yerevan, Armenia*

(Received 4 May 2001; published 8 November 2001)

Spin transfer in deep-inelastic  $\Lambda$  electroproduction has been studied with the HERMES detector using the 27.6 GeV polarized positron beam in the DESY HERA storage ring. For an average fractional energy transfer  $\langle z \rangle = 0.45$ , the longitudinal spin transfer from the virtual photon to the  $\Lambda$  has been extracted. The spin transfer along the  $\Lambda$  momentum direction is found to be  $0.11 \pm 0.17(\text{stat}) \pm 0.03(\text{syst})$ ; similar values are found for other possible choices for the longitudinal spin direction of the  $\Lambda$ . This result is the most precise value obtained to date from deep-inelastic scattering with charged lepton beams, and is sensitive to polarized up quark fragmentation to hyperon states. The experimental result is found to be in general agreement with various models of the  $\Lambda$  spin content, and is consistent with the assumption of helicity conservation in the fragmentation process.

DOI: 10.1103/PhysRevD.64.112005

PACS number(s): 13.60.Rj, 13.87.Fh, 13.88.+e, 25.30.Dh

Spin-dependent deep-inelastic scattering of charged leptons has provided precise information on the spin structure of the nucleon. Several inclusive experiments on polarized proton and neutron targets [1–6] have confirmed the European Muon Collaboration (EMC) result [7], from which it was inferred that the quark spins account for only a small fraction of the nucleon spin. Additional information has been obtained from semi-inclusive polarized deep-inelastic scattering experiments, where the correlation between the flavor of the struck quark and the type of hadron observed in the final state allows the separation of the spin contributions of the various quark flavors and of valence and sea quarks [8,9]. Those measurements indicate that the net contribution of the up and down sea quarks to the nucleon spin is small. However, considerable uncertainties remain in the contributions of strange quarks and gluons.

It has been proposed that one could obtain additional information on the polarized quark distributions in the baryons of the spin 1/2 octet through the production of  $\Lambda$  hyperons in polarized deep-inelastic lepton scattering [10,11]. By measuring the polarization of the  $\Lambda$ 's that are likely to have originated from the struck quark (so-called “current fragmentation”), the longitudinal spin transfer  $D_{LL}^\Lambda$  can be determined. This quantity is defined as the fraction of the virtual photon polarization transferred to the  $\Lambda$ . In the naive quark parton model (QPM) the spin of the  $\Lambda$  is entirely due to the strange quark, and the up and down quark polarizations are zero. On the other hand, assuming SU(3) flavor symmetry, the up, down and strange quark distributions (and fragmentation functions) for the  $\Lambda$  can be related to those in the proton. If existing data on hyperon decays and polarized structure functions of the nucleon are interpreted in the framework of SU(3) symmetry, the first moments of the polarized up and down quark distributions in the  $\Lambda$  can be estimated to be about -0.2 each [10]. If one assumes in addition that quark helicity is conserved in the fragmentation process, one obtains this same negative value for the expected spin transfer from a struck up or down quark to the  $\Lambda$ . A measurement of the spin transfer thus has the potential to provide information on the spin structure of the  $\Lambda$  hyperon.

Longitudinal spin transfer in  $\Lambda$  production has previously been studied at the  $Z^0$  pole at CERN  $e^+e^-$  collider LEP. In the standard model, strange quarks (or quarks of charge -1/3 in general) produced via  $Z^0$  decays have an average polarization of -0.91. Both the ALEPH [12] and OPAL Collaborations [13] have reported a measurement of the  $\Lambda$  polarization of about -0.3 for  $z > 0.3$ . (Here,  $z$  is the fraction of the available energy carried by the  $\Lambda$ .) The interpretation of these data is not unique. In Ref. [14], for example, the LEP data have been confronted with three different scenarios, all of which describe the results reasonably well: the naive QPM of the  $\Lambda$  spin structure, where only the strange quark carries the spin and contributes to polarized  $\Lambda$  production (subsequently referred to as scenario 1), the SU(3) flavor-symmetric model, in which up and down quarks also contribute with a negative sign (scenario 2), and a rather extreme hypothesis, in which all three light quark flavors contribute equally to the  $\Lambda$  polarization (scenario 3). An alternative approach may be found in the work of [15,16] where calculations of the parton distribution functions in the  $\Lambda$  have been performed in various models. Predictions are then made for the  $\Lambda$  spin transfer. These predictions display a marked  $z$  dependence which is directly related to the behavior of the parton distribution functions in the  $\Lambda$  at large  $x$ . In Ref. [16], the LEP data are found to agree well with the prediction, but only if SU(3) symmetry breaking effects are taken into account. A third approach is presented in the LEP publications [12,13]. Following the prescription of [17], the contribution of heavier hyperon decays to the  $\Lambda$  spin transfer was carefully considered. When a  $\Lambda$  is produced from the decay of another hyperon (such as the  $\Sigma^*$ ), its polarization will reflect that of its parent; the resulting spin transfer from the initial “struck” quark to the  $\Lambda$  through this channel will thus be related to the spin structure of the  $\Sigma^*$  rather than the  $\Lambda$ . In the LEP analyses, the fractions of  $\Lambda$  baryons arising from various decay channels were estimated using Monte Carlo simulations in the Lund fragmentation model, and then combined with the naive QPM values for the quark polarization in the various hyperons. The resulting prediction was found to agree well with the data, with up to 50% of the spin transfer arising from heavier hyperon decays. The influence of the heavier hyperons complicates any simple interpretation of the spin transfer in terms of the  $\Lambda$  spin structure alone; in-

\*Deceased.

stead, the data must be viewed in the context of models describing the spin structure of the several hyperons involved. In particular, the  $z$  dependence of the spin transfer needs to be considered, since the influence of heavy hyperon decays will diminish as  $z \rightarrow 1$ .

In the  $e^+e^-$  experiments at LEP, all three light quark flavors contributed significantly to the production of  $\Lambda$  hyperons, with the strange quark playing the dominant role. By contrast,  $\Lambda$  production in deep-inelastic lepton scattering is dominated by scattering on up quarks. Hence such experiments provide a means to distinguish between the various models of the  $\Lambda$  spin structure, and to investigate further the degree of helicity conservation in the fragmentation process.

The polarization of  $\Lambda$  hyperons can be measured via the weak decay channel  $\Lambda \rightarrow p \pi^-$ , through the angular correlation of the final state

$$\frac{dN_p}{d\Omega} \propto 1 + \alpha \vec{P}_\Lambda \cdot \hat{p}. \quad (1)$$

Here  $\alpha = 0.642 \pm 0.013$  is the asymmetry parameter of the parity-violating weak decay,  $\vec{P}_\Lambda$  is the polarization of the  $\Lambda$ , and  $\hat{p}$  is the unit vector along the proton momentum in the rest frame of the  $\Lambda$ . For a longitudinally polarized lepton beam and an unpolarized target, the  $\Lambda$  polarization is given in the quark parton model by [11,18]

$$\vec{P}_\Lambda = \hat{q} P_B D(y) \frac{\sum_f e_f^2 q_f^N(x, Q^2) G_{1,f}^\Lambda(z, Q^2)}{\sum_f e_f^2 q_f^N(x, Q^2) D_{1,f}^\Lambda(z, Q^2)}, \quad (2)$$

where  $P_B$  is the polarization of the charged lepton beam,  $-Q^2$  is the squared four-momentum transfer of the virtual photon with energy  $\nu$ , and  $x = Q^2/2M\nu$  is the Björken scaling variable (with  $M$  denoting the proton mass). The fractional energy transferred to the nucleon is  $y = \nu/E$  (where  $E$  is the lepton beam energy),  $z = E_\Lambda/\nu$  is the energy fraction of the  $\Lambda$ , and  $D(y) \approx y(2-y)/[1+(1-y)^2]$  is the virtual photon depolarization factor. Finally,  $q_f^N(x, Q^2)$  is the quark distribution for flavor  $f$  in the nucleon,  $D_{1,f}^\Lambda(z, Q^2)$  is the spin-independent fragmentation function for  $\Lambda$  production from quark flavor  $f$ ,  $G_{1,f}^\Lambda(z, Q^2)$  is the corresponding longitudinal spin-transfer fragmentation function, and  $e_f$  is the quark charge in units of the elementary charge  $e$ . The symbol  $\hat{q}$  represents the unit vector along the virtual photon direction. The  $\Lambda$  polarization may in general be directed along some other axis  $\hat{L}'$ , such as the  $\Lambda$  momentum [18] or the lepton beam momentum [11]. However, as  $\Lambda$  production at the kinematics of the HERMES experiment may be treated as an essentially collinear process, the effects of such complexities should be small.

Following Ref. [11] the component of the longitudinal spin transfer to the  $\Lambda$  along a longitudinal spin quantization axis  $L'$  is defined as

$$D_{LL'}^\Lambda \equiv \frac{\vec{P}_\Lambda \cdot \hat{L}'}{P_B D(y)} = \frac{\sum_f e_f^2 q_f^N(x, Q^2) G_{1,f}^\Lambda(z, Q^2)}{\sum_f e_f^2 q_f^N(x, Q^2) D_{1,f}^\Lambda(z, Q^2)}, \quad (3)$$

where the subscripts  $L$  and  $L'$  denote the fact that the spin is transferred from a polarized photon to a polarized  $\Lambda$  and that the two longitudinal spin quantization axes may be different. Due to the charge factor for the up quark, the spin transfer in  $\Lambda$  electroproduction is dominated by the spin transfer from the up quark to the  $\Lambda$ . Moreover, due to isospin symmetry the spin transfer coefficients from the up and down quarks to the  $\Lambda$  are expected to be equal. Thus Eq. (3) can be approximated by

$$D_{LL'}^\Lambda \approx \frac{G_{1,u}^\Lambda(z, Q^2)}{D_{1,u}^\Lambda(z, Q^2)}. \quad (4)$$

Consequently,  $\Lambda$  electroproduction in the current fragmentation region is most sensitive to the ratio  $G_{1,u}^\Lambda/D_{1,u}^\Lambda \sim G_{1,d}^\Lambda/D_{1,d}^\Lambda$ . Since the  $Q^2$  range of the measurement reported here is small, it is assumed that  $D_{LL'}^\Lambda$  depends only on the energy fraction  $z$ . If the fragmentation process does indeed possess some degree of helicity conservation between the struck quark and the final state hyperon (as supported by the non-zero  $\Lambda$  polarization observed at LEP), the ratio  $G_{1,u}^\Lambda/D_{1,u}^\Lambda$  should be related to the polarization  $\Delta u^\Lambda/u^\Lambda$  of the up quark in the  $\Lambda$ . If a significant fraction of the  $\Lambda$ 's are produced from the decays of heavier hyperons, then the ratio  $G_{1,u}^\Lambda/D_{1,u}^\Lambda$  will be related instead to a linear combination of the  $u$  quark polarizations in the various hyperons involved.

The measurement was carried out by the HERMES experiment at DESY using the 27.6 GeV polarized positron beam of the HERA storage ring. At HERA, the positrons become transversely polarized by the emission of synchrotron radiation [19]. Longitudinal polarization of the positron beam at the interaction point is achieved with spin rotators [20] situated upstream and downstream of the HERMES experiment. Equilibrium polarization values in the range of 0.40 to 0.65 are reached with a rise time of about 20 min. The beam polarization is continuously measured using Compton backscattering of circularly polarized laser light. The statistical accuracy of this measurement is typically 1% in 60 s; its systematic uncertainty is 3.4%, dominated by the normalization uncertainty determined from the rise-time calibration [21,22]. The beam helicity was reversed between the two years of data acquisition. The data for this analysis are combined from two three-week running periods, one in each of 1996 and 1997, which were dedicated to measurements with unpolarized targets of hydrogen, deuterium,  $^3\text{He}$  and nitrogen with a typical target density of around  $1 \times 10^{15}$  nucleons/cm $^2$ .

A detailed description of the HERMES spectrometer is provided in Ref. [23]. The trajectories of the particles are determined in the region in front of the spectrometer magnet by a set of two drift chambers, and the momenta are deter-

mined by matching these to tracks in two sets of drift chambers in the back region behind the magnet. In addition there are three proportional chambers inside the magnet to track low momentum particles that do not reach the rear section of the spectrometer. Particle identification is accomplished using a lead glass calorimeter, a scintillator hodoscope preceded by two radiation lengths of lead, a transition radiation detector, and a  $C_4F_{10}/N_2$  (30:70) gas threshold Čerenkov counter. Combining the responses of these detectors in a likelihood method leads to an average positron identification efficiency of 99%, with a hadron contamination of less than 1%. In addition, the Čerenkov counter is used to distinguish pions from heavier hadrons for momenta between 4.5 and 13.5 GeV.

Semi-inclusive  $\Lambda$  events were selected by requiring at least three reconstructed tracks: a positron track in coincidence with two hadron candidate tracks of opposite charge. Both the track of the scattered positron and that of the positive hadron candidate are always reconstructed using all drift chambers and all particle identification detectors. The negative hadron candidate is allowed to have only partial track information. These partial tracks are reconstructed by the drift chambers in the front region and by the wire chambers located in the magnet region. In this way it is possible to get momentum and charge information from these tracks, though no information from the particle identification and drift chambers in the back portion of the spectrometer exists. As almost all negative particles are pions, particle identification is not essential for these tracks. In this analysis, the track resolution at HERMES is dominated by the resolution of the drift chambers in front of the magnet. Thus the resolution of the partial tracks does not differ significantly from that of the full tracks. An invariant mass is reconstructed assuming that the positive hadron is a proton and the negative hadron is a pion. If more than one positive or negative hadron exists in one event, all possible pairings of positive and negative hadrons are used.

Several requirements were imposed to ensure that the events are in the deep-inelastic scattering region and to reduce the background in the semi-inclusive  $\Lambda$  sample:  $Q^2 > 1 \text{ GeV}^2$ ,  $W > 2 \text{ GeV}$ , and  $y < 0.85$ , the latter to avoid a region where radiative corrections might be significant. Here  $W$  is defined as the invariant mass of the photon-nucleon system. The calorimeter energy deposited by the scattered positron was required to be greater than 4 GeV, well above the trigger threshold of 3.5 GeV. To ensure that the event occurred in the target gas, the longitudinal vertex position of the positron track was constrained to be within the total length of the target cell ( $\pm 20 \text{ cm}$  from the center of the target). The positron interaction vertex and the  $\Lambda$  decay vertex were required to be separated by more than 10 cm to eliminate background hadrons originating from the primary vertex. Additionally, the distance of closest approach between the two hadron tracks was required to be less than 1.5 cm. The collinearity, defined as the cosine of the angle between the  $\Lambda$  momentum (computed from the proton and pion momenta) and the  $\Lambda$  direction of motion (computed from the vector displacement between the positron vertex and the  $\Lambda$  decay vertex), was required to be above 0.998. To reduce the

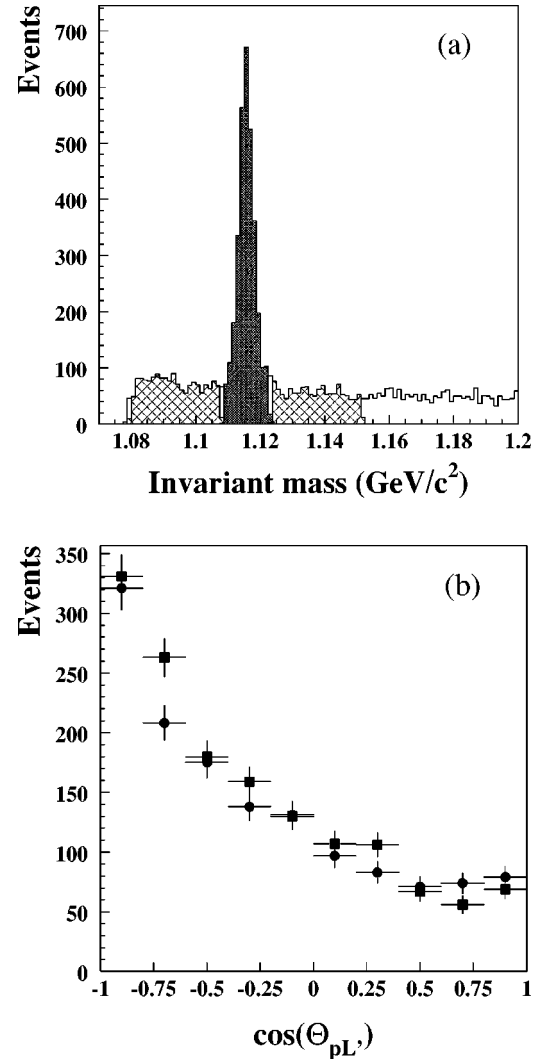


FIG. 1. (a) Invariant mass spectrum from the reconstruction of candidate  $\Lambda$  events. The filled and hatched areas, respectively, indicate the signal and background regions used in the analysis. (b) Spectrum of  $\cos \Theta_{pL'}$  for the two beam helicities (circles and squares). The asymmetric appearance of these spectra is almost entirely due to the acceptance of the HERMES spectrometer for reconstructing  $\Lambda$  decays.

large pion contribution to the positive hadron sample, the positive hadron was required to have no Čerenkov signal. Finally, to ensure that the  $\Lambda$  hyperons are primarily from the current fragmentation region, a positive value of  $x_F \approx 2p_L/W$  was required. Here  $p_L$  is the momentum component of the  $\Lambda$  that is longitudinal with respect to the virtual photon in the photon-nucleon center-of-mass frame. After all these criteria have been implemented, a clean  $\Lambda$  signal is observed in the invariant mass distribution [see Fig. 1(a)].  $\Lambda$  events have been selected by a cut on the invariant mass distribution:  $1.109 \text{ GeV} < M_{p\pi} < 1.123 \text{ GeV}$ , resulting in a total number of 2237  $\Lambda$  events (after background subtraction).

As the HERMES spectrometer is a forward detector, its acceptance for the reconstruction of  $\Lambda$  hyperons is limited and strongly depends on  $\cos \Theta_{pL'}$  [see Fig. 1(b)]. Here  $\Theta_{pL'}$

is the angle between the proton momentum and the  $\Lambda$  spin quantization axis in the rest frame of the  $\Lambda$ . To minimize acceptance effects, the spin transfer to the  $\Lambda$  has been determined by combining the two data sets measured with opposite beam helicities in such a way that the luminosity-weighted average beam polarization for the selected data sample is zero. Using this data sample and assuming that the spectrometer acceptance did not change between the two beam helicity states, the spin transfer to the  $\Lambda$  is determined from the forward-backward asymmetry in the angular distributions in  $\Lambda$  electroproduction [24,25]:

$$D_{LL'}^\Lambda = \frac{1}{\alpha \langle P_B^2 \rangle} \frac{\sum_{i=1}^{N_\Lambda} P_{B,i} \cos \Theta_{pL'}^i}{\sum_{i=1}^{N_\Lambda} D(y_i) \cos^2 \Theta_{pL'}^i}. \quad (5)$$

The indicated sums are over the  $\Lambda$  events, and  $\langle P_B^2 \rangle$  is the luminosity-weighted average of the square of the beam polarization. The extracted quantity  $D_{LL'}$  represents the component of the spin transfer coefficient along a chosen quantization axis  $L'$ , which has been taken to be parallel to the direction of motion of the  $\Lambda$  baryon. As mentioned earlier, the two similar directions that have also been considered in this analysis may be considered equivalent hypotheses for the true direction of the  $\Lambda$  polarization, given the collinear nature of the process at the kinematics of this experiment. In addition, the derivation of Eq. (5) requires that there is no correlation among the kinematic variables, i.e., between  $y$  and  $\cos \Theta_{pL'}$ . This has been verified for this data set.

Equation (5) provides a simple method to extract  $D_{LL'}$ , without any influence from the spectrometer acceptance, from a cross section of the form

$$\frac{dN_p}{d\Omega} \propto 1 + \alpha P_B D(y) D_{LL'} \cos \Theta_{pL'}. \quad (6)$$

However, this form of the cross section presupposes that the selected spin quantization axis  $L'$  is indeed the direction of the  $\Lambda$  polarization. In general, other components of the polarization may exist. In this case, the extracted result for  $D_{LL'}$  may be contaminated by interference of certain additional terms in the cross section with higher-order terms in the HERMES angular acceptance (see the Appendix). However, Monte Carlo studies reveal that even if these other components of the polarization were of the same magnitude as  $D_{LL'}$ , they would contribute to the result presented here at a level of less than 10% of the extracted value.

After applying all the requirements described above, the longitudinal spin transfer to the  $\Lambda$  was extracted using Eq. (5). As no nuclear effects were observed within the limited statistics of this measurement, the data collected on the various targets ( $^1\text{H}$ ,  $^2\text{H}$ ,  $^3\text{He}$ , and  $^{14}\text{N}$ ) have been added. To minimize possible acceptance-induced false asymmetries, the data have been corrected for the difference in tracking efficiencies between the two years by normalizing the number of  $\Lambda$  events to the number of all events where two hadrons and a scattered positron were reconstructed. The spin

transfer  $D_{LL'}^\Lambda$ , due to background events in the selected invariant mass region has been determined from the events above and below the  $\Lambda$  invariant mass region [indicated by the hatched areas in Fig. 1(a)]. It was found to be consistent with zero and has been taken into account as a dilution. At an average  $z$  value of 0.45 the spin transfer to the  $\Lambda$  is found to be  $D_{LL'}^\Lambda = 0.11 \pm 0.17(\text{stat}) \pm 0.03(\text{sys})$ , using the  $\Lambda$  momentum as the spin quantization axis  $L'$ . If instead the virtual photon (positron beam) momentum is chosen as quantization axis, the result changes to 0.03(0.09) with the same uncertainties. Equations (2) and (3) are based on the assumption that the  $\Lambda$  hyperons originate from the current fragmentation region. Contributions from the target fragmentation region are suppressed by the requirement  $x_F > 0$  and have been estimated by a Monte Carlo simulation to be smaller than 1%. The data cover a  $z$  range of  $0.2 < z < 0.7$ , with  $x$  values of  $0.02 < x < 0.4$ , and with  $Q^2$  varying between 1 and 10  $\text{GeV}^2$ . The average values of these kinematic variables are  $\langle z \rangle = 0.45$ ,  $\langle x \rangle = 0.08$ , and  $\langle Q^2 \rangle = 2.5 \text{ GeV}^2$ . The systematic uncertainty of the measurement is dominated by the uncertainties in detector efficiency differences between the two data sets. Possible efficiency differences due to the different kinematic distributions of the  $\Lambda$  decay products and of two reconstructed hadrons in any event have been explored and found to be negligible. Finally, possible false asymmetries induced by changes in the detector performance between the two years were investigated using both Monte Carlo simulations and samples of hadron pairs outside the  $\Lambda$  mass peak. No significant asymmetries were found by these studies.

The three models of Ref. [14] for the  $\Lambda$  spin structure (mentioned earlier in comparison to the LEP data) have been used to predict the  $z$  dependence of the spin transfer in  $\Lambda$  electroproduction. In contrast to the LEP data, the deep-inelastic scattering (DIS) measurements are dominated by scattering from up quarks and can thus impose different constraints on the various  $\Lambda$  spin structure scenarios. Figure 2 shows a comparison of the present measurement with these predictions. Following Ref. [14] the data are not given at  $z = E_\Lambda / \nu$  but at  $z' \equiv E_\Lambda / [E_N(1-x)]$ , a variable that accounts for the small contamination by target fragmentation. Here  $E_\Lambda$  and  $E_N$  are the energies of the  $\Lambda$  and nucleon, respectively, in the photon-nucleon center of mass system. Also shown in the figure is a measurement at a similar  $z$  value from the E665 Collaboration [26], using DIS with a polarized muon beam. The E665 measurement is also similar in its average  $Q^2$  value ( $\langle Q^2 \rangle = 1.3 \text{ GeV}^2$ ) but is at much lower  $x$  ( $\langle x \rangle = 0.005$ ) than the measurement presented here ( $\langle x \rangle = 0.08$ ). Further, a recent measurement in  $\nu_\mu$  charged current interactions [27] has shown a  $\Lambda$  polarization close to zero in the current fragmentation region, in agreement with our finding for the  $\Lambda$  spin transfer. This measurement is also dominated by  $\Lambda$  production from polarized up quarks.

Figure 2 indicates that the HERMES measurement appears to favor the naive QPM of the  $\Lambda$  spin structure (scenario 1). However, as discussed earlier, a significant complication arises from the fact that  $\Lambda$  hyperons may originate from decays of heavier hyperons. A Monte Carlo estimate shows that only 40–50 % of the  $\Lambda$ 's are produced directly;

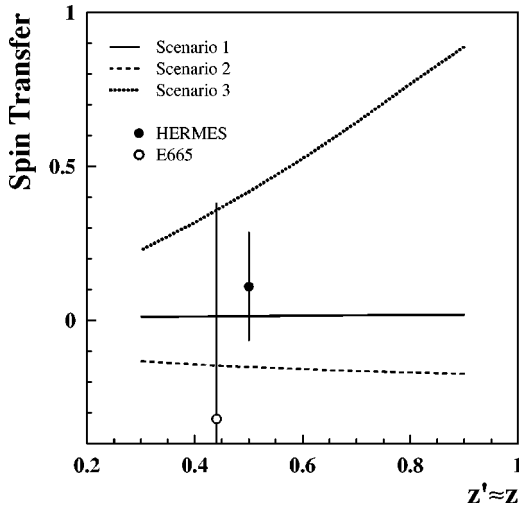


FIG. 2. Spin transfer  $D_{LL'}^\Lambda$  as a function of  $z' = E_\Lambda/E_N(1-x)$  for the spin quantization axis  $L'$  along the  $\Lambda$  momentum. The error bar represents the quadratic sum of statistical and systematic uncertainties. The curves correspond to various models for the  $\Lambda$  spin structure from Ref. [14]: the naive QPM (scenario 1), the SU(3) flavor-symmetric model (scenario 2), and a model with equal contributions of all light quark flavors to the  $\Lambda$  polarization (scenario 3).

30–40 % originate from  $\Sigma^*(1385)$  decay, and about 20% are decay products of the  $\Sigma^0$ . The up quarks in the  $\Sigma^*$  are expected to carry a significant positive polarization. Polarized up quarks from the target will thus tend to fragment into  $\Sigma^*$  hyperons with a positive spin transfer coefficient, which is then passed on to the  $\Lambda$  polarization through the decay. The  $\Sigma^0$  is of lesser influence, making a smaller contribution of opposite sign to the  $\Lambda$  polarization. The net contribution of  $\Sigma$  decays to the  $\Lambda$  sample will thus shift the negative prediction of the SU(3) symmetric model (scenario 2), along with that of the naive QPM (scenario 1), toward positive values. This effect is also observed at the kinematics of the E665 experiment, as can be seen in Ref. [28].

As pointed out in Ref. [14], strong contributions from the decays of heavier hyperons provide one possible cause for the positive spin transfer values of scenario 3. Also, large positive values for the spin transfer at high  $z$  are expected in models where the polarization of each quark flavor is expected to be large in the limit  $x \rightarrow 1$  [29,16]: via the Gribov-Lipatov reciprocity relation [30], the large quark polarization at  $x=1$  produces a large spin transfer at  $z=1$ . The present HERMES result cannot yet distinguish between these various models. Additional data will significantly improve the precision, and should allow access to higher values of  $z$  where contributions from heavier hyperons are reduced and where the various models predict markedly different results.

In conclusion, HERMES has measured the longitudinal spin transfer from the virtual photon to the  $\Lambda$  hyperon in deep-inelastic electroproduction, finding the value  $D_{LL'} = 0.11 \pm 0.17(\text{stat}) \pm 0.03(\text{syst})$  at an average fractional energy transfer of  $\langle z \rangle = 0.45$ . This result is complementary to measurements from  $e^+e^-$  annihilation, as it is uniquely sensitive to the fragmentation of polarized  $up$  quarks. The result

is in general agreement with calculations based on a variety of models of the  $\Lambda$  spin structure, along with the hypothesis of significant helicity conservation in the fragmentation process (as suggested by earlier data from LEP). Forthcoming data from HERMES will improve the precision of the measurement, and help both to explore the  $\Lambda$  spin structure and to further test the degree of helicity conservation in the final state.

## ACKNOWLEDGMENTS

We gratefully acknowledge the DESY management for its support and the DESY staff and the staffs of the collaborating institutions. This work was supported by the FWO-Flanders, Belgium; the Natural Sciences and Engineering Research Council of Canada; the INTAS, HCM, and TMR network contributions from the European Community; the German Bundesministerium für Bildung und Forschung; the Deutscher Akademischer Austauschdienst (DAAD); the Italian Istituto Nazionale di Fisica Nucleare (INFN); Monbusho, JSPS, and Toary Science Foundation of Japan; the Dutch Foundation for Fundamenteel Onderzoek der Materie (FOM); the U.K. Particle Physics and Astronomy Research Council; and the U.S. Department of Energy and National Science Foundation.

## APPENDIX

As described above, the procedure used to extract the longitudinal spin transfer coefficient  $D_{LL'}$  [Eq. (5)] is based on the assumption that the selected spin quantization axis  $L'$  is indeed the direction of the  $\Lambda$  polarization. However, if other components of the polarization exist, the extracted result for  $D_{LL'}$  may be contaminated via interference of certain additional terms in the cross section with higher-order terms in the HERMES angular acceptance.

Let us introduce 3 perpendicular axes in the  $\Lambda$  center of mass frame, defined by two chosen unit vectors  $\hat{J}$  and  $\hat{T}$ :  $\hat{e}_1 \equiv \hat{J}$ ,  $\hat{e}_2 \equiv \hat{J} \times \hat{T} / |\hat{J} \times \hat{T}|$ ,  $\hat{e}_3 \equiv \hat{e}_1 \times \hat{e}_2$ . Further, let the symbol  $D_{Li}$  refer to the probability for spin transfer from a longitudinally polarized virtual photon to a  $\Lambda$  baryon with polarization along the axis  $i$ ; the symbol  $D_{Ui}$  denotes the probability for  $\Lambda$  polarization along the axis  $i$  given an unpolarized beam. We take the vector  $\hat{J}$  to represent our direction of interest for longitudinal spin transfer to the  $\Lambda$ , namely the direction of the virtual photon. The quantity  $D_{L1}$  is thus identical to the quantity  $D_{LL'}$  defined previously [Eq. (3)]. The vector  $\hat{T}$  may be either of the other two vectors available: the electron beam direction or the momentum of the final state  $\Lambda$ . The second axis  $\hat{e}_2$  thus represents the direction normal to the production plane. The number of interfering terms is greatly restricted by applying parity and rotational invariance to a general angular decomposition of the cross section, and by the fact that the HERMES spectrometer is symmetric in the vertical coordinate. Finally one is left with only two terms:

$$\alpha D_{U2} \cos \Theta_2 [P_B \sin(n\Phi)] \quad (\text{A1})$$

and

$$\alpha P_B D(y) D_{L3} \cos \Theta_3 [1 + C_n \cos(n\Phi)]. \quad (\text{A2})$$

In obtaining these expressions, it is important to note that the axis  $\hat{e}_2$ , which represents the direction normal to the reaction plane, transforms as a pseudo-vector, while  $\hat{e}_1$  and  $\hat{e}_3$  transform as vectors. The first contribution [Eq. (A1)] depends entirely on a non-zero  $P_B \sin(n\Phi)$  azimuthal moment in  $\Lambda$  production, where  $\Phi$  denotes the angle between the  $\Lambda$  and

the electron scattering plane, around the  $\vec{q}$  vector. Such moments have been measured to be small in pion production. In addition, they are coupled here with a transverse  $\Lambda$  polarization and can only appear in the cross section at higher twist (i.e., they are suppressed at order  $p_T/Q$ ). The second term [Eq. (A2)] corresponds to the other component of  $\Lambda$  spin transfer in the production plane, and could contribute if the chosen spin quantization axis differs dramatically from the true  $\Lambda$  polarization direction. Monte Carlo studies reveal that even if either of the coefficients  $D_{U2}$  or  $D_{L3}$  were of the same magnitude as  $D_{L1}$ , they would contribute to the extracted component at a level of less than 10% of its value.

- 
- [1] E142 Collaboration, P. L. Anthony *et al.*, Phys. Rev. D **54**, 6620 (1996).
- [2] E143 Collaboration, K. Abe *et al.*, Phys. Rev. Lett. **74**, 346 (1995); Phys. Lett. B **364**, 61 (1995); Phys. Rev. D **58**, 112003 (1998).
- [3] SMC Collaboration, D. Adams *et al.*, Phys. Lett. B **329**, 399 (1994); Phys. Rev. D **56**, 5330 (1997); B. Adeva *et al.*, Phys. Lett. B **412**, 414 (1997); Phys. Rev. D **58**, 112001 (1998).
- [4] E154 Collaboration, K. Abe *et al.*, Phys. Rev. Lett. **79**, 26 (1997).
- [5] HERMES Collaboration, K. Ackerstaff *et al.*, Phys. Lett. B **404**, 383 (1997).
- [6] HERMES Collaboration, A. Airapetian *et al.*, Phys. Lett. B **442**, 484 (1998).
- [7] EMC Collaboration, J. Ashman *et al.*, Nucl. Phys. **B328**, 1 (1989).
- [8] SMC Collaboration, B. Adeva *et al.*, Phys. Lett. B **420**, 180 (1998).
- [9] HERMES Collaboration, K. Ackerstaff *et al.*, Phys. Lett. B **464**, 123 (1999).
- [10] M. Burkardt and R. L. Jaffe, Phys. Rev. Lett. **70**, 2537 (1993).
- [11] R. L. Jaffe, Phys. Rev. D **54**, R6581 (1996), and references therein.
- [12] ALEPH Collaboration, D. Buskulic *et al.*, Phys. Lett. B **374**, 319 (1996).
- [13] OPAL Collaboration, K. Ackerstaff *et al.*, Eur. Phys. J. C **2**, 49 (1998).
- [14] D. de Florian, M. Stratman, and W. Vogelsang, Phys. Rev. D **57**, 5811 (1998).
- [15] B.-Q. Ma, I. Schmidt, and J.-J. Yang, Phys. Rev. D **61**, 034017 (2000).
- [16] C. Boros, J. T. Londergan, and A. W. Thomas, Phys. Rev. D **61**, 014007 (2000).
- [17] G. Gustafson and J. Hakkinen, Phys. Lett. B **303**, 350 (1993).
- [18] P. J. Mulders and R. D. Tangerman, Nucl. Phys. **B461**, 197 (1996), and references therein.
- [19] A. A. Sokolov and I. M. Ternov, Sov. Phys. Dokl. **8**, 1203 (1964).
- [20] D. P. Barber *et al.*, Phys. Lett. B **343**, 436 (1995).
- [21] D. P. Barber *et al.*, Nucl. Instrum. Methods Phys. Res. A **329**, 79 (1993).
- [22] A. Most, in *Proceedings of the 12th International Symposium on High-Energy Spin Physics*, edited by C. W. de Jager *et al.* (World Scientific, Amsterdam, The Netherlands, 1997), p. 800.
- [23] HERMES Collaboration, K. Ackerstaff *et al.*, Nucl. Instrum. Methods Phys. Res. A **417**, 230 (1998).
- [24] S. Belostotski, HERMES internal report 98-091 (available as HERMES internal note, and can be accessed on the HERMES web pages: <http://hermes.desy.de/notes/>).
- [25] G. Schnell, Ph.D. thesis, New Mexico State University, 1999 (available as HERMES internal note, and can be accessed on the HERMES web pages: <http://hermes.desy.de/notes/>).
- [26] E665 Collaboration, M. R. Adams *et al.*, Eur. Phys. J. C **17**, 263 (2000).
- [27] NOMAD Collaboration, P. Astier *et al.*, Nucl. Phys. **B588**, 3 (2000).
- [28] D. Ashery and H. J. Lipkin, Phys. Lett. B **469**, 263 (1999).
- [29] B.-Q. Ma, I. Schmidt, and J.-J. Yang, Phys. Lett. B **477**, 107 (2000); B.-Q. Ma *et al.*, Eur. Phys. J. C **16**, 657 (2000).
- [30] V. N. Gribov and L. N. Lipatov, Phys. Lett. **37B**, 78 (1971); Sov. J. Nucl. Phys. **15**, 675 (1972).